Feedback between deglaciation and volcanic emissions of CO_2

Peter Huybers[a] & Charles Langmuir[b]

Department of Earth and Planetary Sciences

Harvard University, Cambridge, MA 02138.

[a] *corresponding author, email: phuybers@fas.harvard.edu*

phone: (617)495-8391, fax: (617) 496-7411.

[b] *email: langmuir@eps.harvard.edu.*

Abstract

The concentration of atmospheric CO_2 has varied in near lock-step with glaciation over the course of at least the late Pleistocene. These glacial/interglacial variations in CO_2 are generally attributed to oceanic mechanisms, but here we present evidence that the vast carbon reservoir associated with the solid Earth also plays an important role. A global reconstruction of volcanic activity between 12 ka to 7 ka shows that the frequency of eruptions increases by a factor of two to six, relative to background eruption rates during the glacial and interglacial. This change is statistically highly significant. Furthermore, the spatial pattern of the increased volcanism coincides with the pattern of ice loss coming out of the last glacial. We estimate that the magnitude of the ice unloading associated with mountain glaciers and ice caps could cause decompressional melting of the mantle well in excess of that need to sustain a factor of six increase in volcanic output for 5 ky. In addition to increased melt production, glacial variability may also pace the timing of low-frequency eruptions so as to coincide with deglaciation, a scenario we illustrate with a simple model.

Assuming that volcanic emissions of CO_2 are proportional to the frequency of eruptions, we calculate that 1000 to 5000 Gt of CO_2 is emitted in addition to the long-term average background flux. After accounting for equilibration with the ocean, the CO_2 flux is consistent in timing and magnitude with ice core observations of a 40 ppm increase in atmospheric CO_2 concentration during the second half of the last deglaciation. Apparently, volcanism forges a link between glacial variability and atmospheric CO_2 concentrations and, thus, constitutes a positive feedback upon deglaciation which contributes to the rapid passage from glacial to interglacial periods. Conversely, waning volcanic activity during an interglacial would contribute to cooling and reglaciation, thus tending to suppress volcanic emissions and promote the onset of an ice age.

1 Introduction

Volcanism fluxes carbon from Earth's interior to its exterior fluid envelope, and links among volcanism, the carbon cycle, and climate have long been recognized to operate at long timescales ($\geq 10^6$ ys) (Walker et al., 1981). Short-term (10^0 ys) changes in climate and weather also results from volcanic eruptions; for example, the 1991 Mount Pinatubo eruption injected enough aerosols into the atmosphere to decrease Earth's surface temperature by half a degree Celsius for about a year (Hansen et al., 1992). Evidence has also accumulated that shot-term changes in weather and environment influence volcanism, and the subtle variation associated with Earth tides (Johntson and Mauk, 1972; Hamilton, 1973; Sparks, 1981), daily variations in atmospheric pressure and temperature (Neuberg, 2000), seasonal changes in water storage (Saar and Manga, 2003; Mason et al., 2004), and other short-term changes in environment (Kennett and Thunell, 1975; Rampino et al., 1979; Dzurisin, 1980) have all been implicated as influencing the timing of volcanic eruptions.

In this paper we explore the relationship between glacial loading, volcanic eruptions, and climate on the intermediate timescales pertinent to glacial/interglacial variations (10^3-10^5 ys). If subtle changes in weather and climate are sufficient to influence the timing of volcanism, it is perhaps no surprise for the massive changes associated with deglaciation to also affect volcanism (Hall, 1982). Indeed, deglaciation is observed to coincide with increased volcanism in Iceland (Jull and Mckenzie, 1996; Maclennan et al., 2002; Sinton et al., 2005; Licciardi et al., 2007), France and Germany (Nowell et al., 2006), eastern California (Jellinik et al., 2004), the Pacific Northwest (Bacon and Lanphere, 2006), and Chile (Best, 1992; Gardeweg et al., 1998). Of these, the most clear demonstration comes from Iceland, where dates from lava flows (Sigvaldason et al., 1992; Jull and Mckenzie, 1996), sulphate concentrations in Greenland ice-cores (Zielinksi et al., 1997), and table mountains (Licciardi et al., 2007) are all consistent with increased volcanism during or following deglaciation. The effect on Iceland has also been modeled as resulting from decompression melting of the mantle caused by removal of an approximately two km thick ice sheet during deglaciation (Jull and Mckenzie, 1996; Maclennan et al., 2002). Furthermore, volcanic eruptions are more likely to occur when the confining pressure associated with magma reservoirs and fluid transport in confining rock is decreased by ice removal.

Observations and some theory thus suggests that deglaciation increases volcanism. In this paper we assess the global extent of changes in volcanism during the last deglaciation and consider the consequences such changes could have on climate, particularly with regard to changes in the concentration of atmospheric CO_2.

2 Volcanic activity through the last deglaciation

To test the global extent and magnitude of increased volcanism during the last deglaciation, we combine together two datasets (Bryson et al., 2006; Siebert and Simkin, 2002) comprising the date (Fig. 1) and location (Fig. 3) of eruptions over the last 40 ky. The dataset from (Siebert and Simkin, 2002) only covers the Holocene, but is more complete over this interval and gives an indication of the size of the eruption using the Volcanic Explosivity Index (VEI). Redundant events between the datasets were removed, as were events without age estimates or which are not bracketed between certain dates. We also exclude small events (VEI$\leq$ 2), unless explicitly stated otherwise, because they are less likely to be consistently identified in the past (Siebert and Simkin, 2002), leaving a total of 5352 volcanic events during the last 40,000 years.

The dates of most volcanic events are uncertain (Siebert and Simkin, 2002), and we use a probability distribution to describe when each occurred. The reported calendar age uncertainties are used for each event or, in the case of radiocarbon, the dates and their uncertainties are adjusted to calendar ages using the CALIB 5.0 program (Stuiver et al., 2005). Ages without a reported uncertainty are assumed to have a normal probability distribution with a standard deviation of ten percent of the age, which is large relative to most dating uncertainties. In this manner, the dataset of 5352 events and their uncertain ages are transformed into an equal number of probability distributions spanning the interval from 40,000 years ago to the present (Fig. 1). The data show a marked observational bias with 80% of the dated eruptions occurring in the

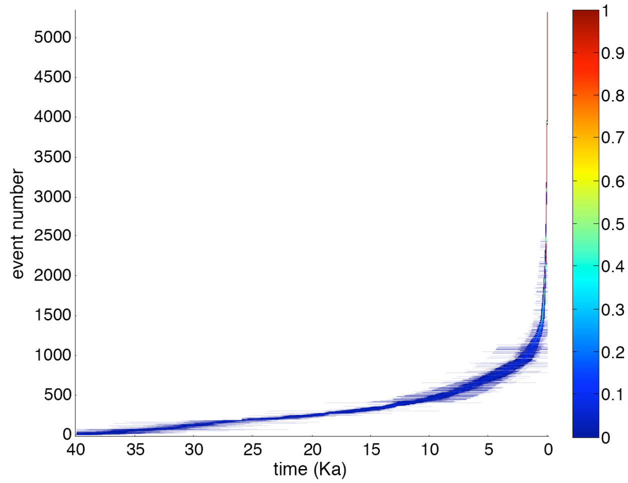

Fig. 1. The timing of volcanic events in the combined databases (Bryson et al., 2006; Siebert and Simkin, 2002) in thousands of years before 1950 AD. Shading indicates the probability that a volcanic event occurred within each 50 year interval between 40 ka and the present. Events are listed in order of the expected time associated with each distribution. Note the observational bias toward recent years: ∼80% of the known and dated events occur within the last 1000 years.

last 1000 years. This temporal bias presents a major challenge to assessing the amount and distribution of volcanism.

2.1 Mapping of volcanic activity

We first explore the spatial distribution of volcanism. If deglaciation has an important causal effect, we expect increased volcanic activity in regions which underwent significant unloading of ice coming out of the last glacial, i.e. primrily at high latitudes and high elevations. To assess this hypothesis, the average frequency of eruptions are mapped during three distinct intervals: the glacial (40-20 ka), the deglacial (17-7 ka), and the late Holocene (5-0 ka). Mapping is accomplished using a time- and space-weighted average, $F(\phi,\theta) = \sum_{i=1}^{N} P_{i,j}\lambda_i$. Here $P_{i,j}$ is the probability that event i occurred during interval j. The spatial-weighting term, $\lambda_i(\phi,\theta) = s/(s+r_i(\phi,\theta))^2$, depends on the distance, r, between each point on the globe (latitude, ϕ, and longitude, θ) and each volcanic event, i. A smoothing length scale, s, of 500 km is used. Regions closest to the largest number of eruptions will have the largest F (see Fig. 2).

The average magnitudes of the mapped volcanic frequencies are strongly influence by the temporal bias against observing older events, and the spatial patterns are also susceptible to observational biases (as we will discuss in more detail later), yet there are a few points which can be made at the outset. The zonal averages associated with the late Holocene and glacial periods can be described, to zero-order, as uniform with latitude. More detailed structure includes a tapering off at high-latitudes and a bulge at low- to mid-northern latitudes during the glacial. The deglacial period, however, has a distinct maximum at high northern latitudes and a smaller maxima at high southern latitudes. These patterns will underlie our attempts to reconstruct volcanic activity, particularly the excess high-latitude activity during the deglaciation.

To circumvent the temporal bias evident in Figs. 1 and 2, we now focus on relative changes in the spatial distribution of volcanic events rather than on the absolute number of events. The ratio of deglacial to glacial eruption frequency at a given location will tend to be greater than one because of the observational bias, but if there is a deglacial increase of volcanism, the ratios will have relatively larger values in regions which underwent significant deglaciation, as is supported by the observations (Fig. 3). Specifically, the Southern Andes (McCulloch et al., 2000), Alaska and the Aleutian Arc (Denton and Hughes, 1981; Yu et al., 2008), the Cascades and Cordillera regions (Denton and Hughes,

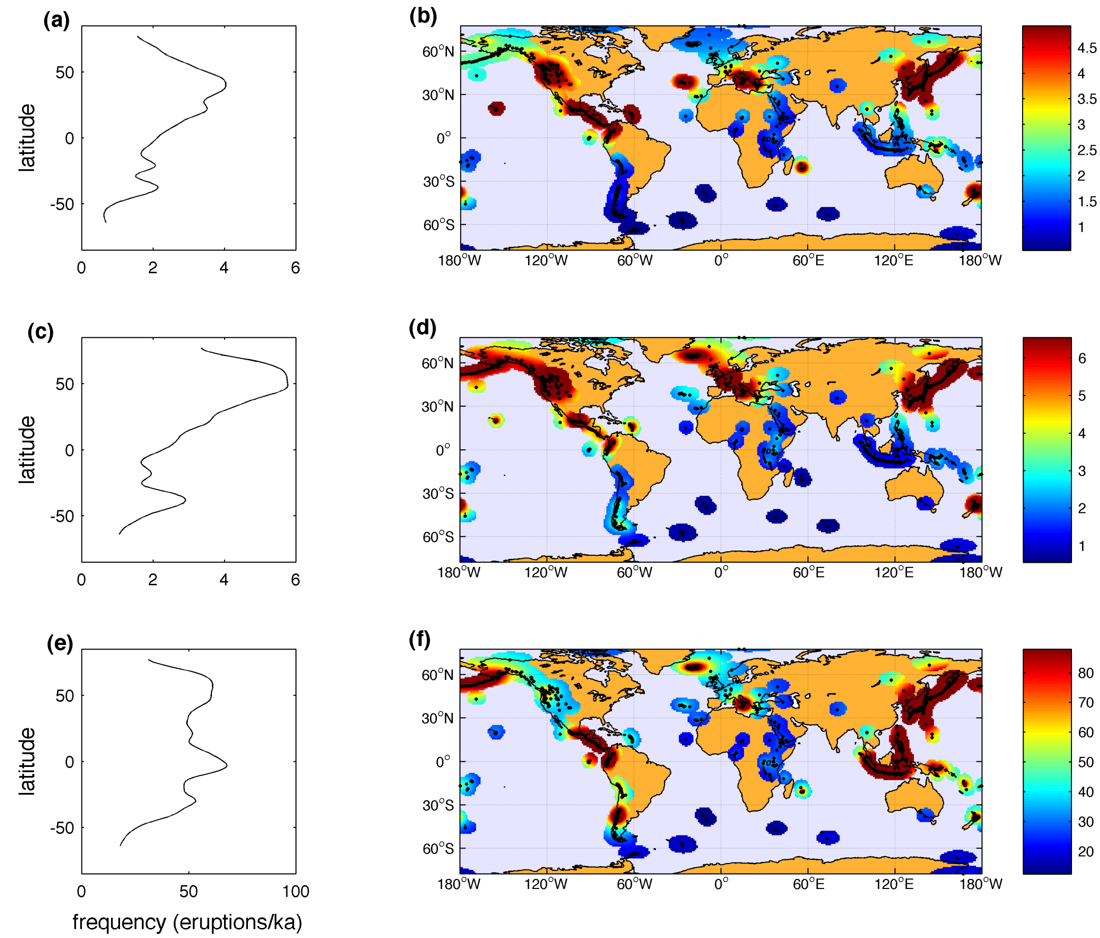

Fig. 2. Patterns of eruption frequency. **(a,b)** Average eruption frequency observed during the glacial (40-20 ka) and the zonal average. Frequencies are only shown in regions within 5° of a volcano (black dots) and are only averaged in these regions. **(c,d)** are similar to (a,b) but for the deglacial (18-7 ka), and **(e,f)** are for the late Holocene (5-0 ka). In order to prevent highly sampled regions from dominating the result, frequencies are capped at two standard deviations above the spatial mean. The zonal averages are smoothed with a tapered window 15° latitude in length. Note that more recent intervals have a higher average frequency and that the deglacial interval shows maxima at high latitudes.

1981; Dyke, 2004), Iceland (Maclennan et al., 2002; Licciardi et al., 2007), Western Europe (Boulton et al., 2001), and possibly Eastern Russia (Grosswald, 1998; Bigg et al., 2008) all experienced significant deglaciation and have high relative eruption frequencies compared to volcanic regions which experienced little ice unloading such as Southeast Asia, Northern New Zealand, Africa, and the tropical Americas.

The interpretation of deglacial/glacial ratios may be confounded by differential preservation of volcanic evidence in glaciated regions. Processes such as ash emplacement atop ice or tephra emplaced and then scoured by ice would tend to destroy evidence of eruptions during the glacial period. If glaciers do significantly hinder preservation and increase erosion, then glaciated regions would be expected to have larger deglacial to glacial ratios. Conversely, glaciated regions would be expected to have a lower deglacial to late-Holocene eruption frequency, owing to decreasing ice coming forward in time. However, the pattern observed for the ratio of deglacial to late-Holocene volcanic frequencies (which are biased toward values less than one, Fig. 3b) is similar to the pattern of deglacial to glacial volcanic frequencies (which are biased toward values greater than one, Fig. 3d). Thus, both ratios show patterns consistent with increased volcanism during deglaciation, even in the face of opposite observational biases.

A simple description of the deglacial pattern can be obtained by taking the zonal average of the frequency ratio. Only points within 5° of a volcano are included in order to focus on active regions. Both the deglacial to glacial (Fig. 3a) and deglacial to late Holocene intervals (Fig. 3c) broadly indicate increased volcanism at high latitudes, consistent with our expectation of greater volcanism in regions experiencing greater deglaciation. Furthermore, ratios are largest at mid and high northern latitudes, coincident with those latitudes experiencing greater glacial unloading.

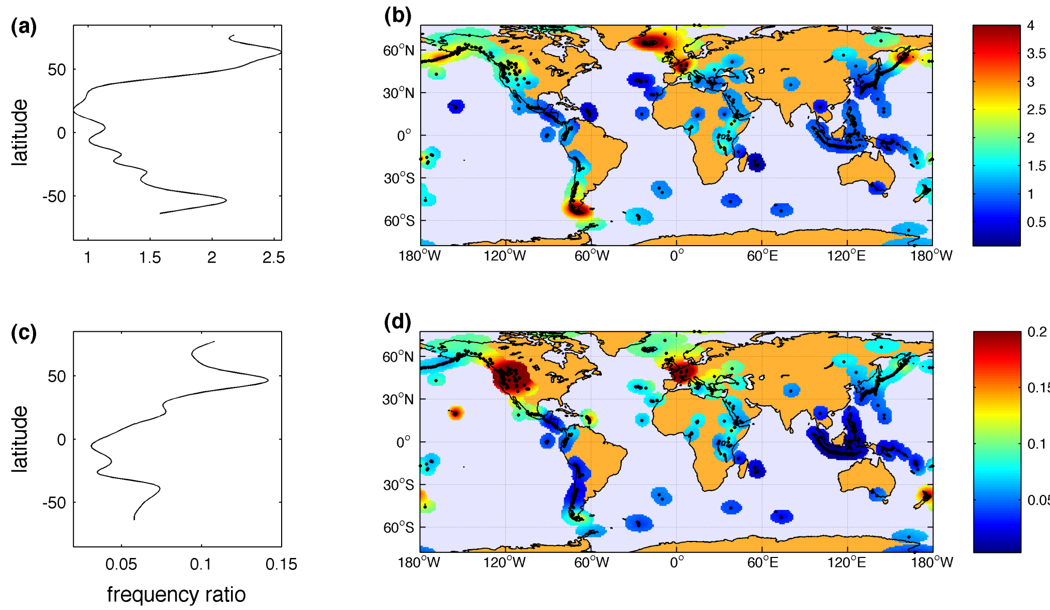

Fig. 3. Relative patterns of eruption frequency during the deglaciation. **(a,b)** Ratios of the average eruption frequency during the deglaciation (17-7 ka) to the eruption frequency during the glacial (40-20 ka) and the zonal average. Frequency ratios are only shown in regions within 5° of a volcano (black dots) and are only averaged in these regions. The temporal reporting bias (see. Fig. 1) causes most ratios to be greater than one. **(c,d)** Similar to (a,b) but the ratio between deglacial (17-7 ka) and late Holocene (5-0 ka) eruption frequencies. All values are less than one because of the temporal bias.

As another check of this approach, we also consider the ratio of glacial to late-Holocene volcanism (not shown), which is strongly susceptible to preservation biases but without either interval containing a major deglaciation episode. This ratio shows no tendency toward systematically high or low values in glaciated regions, indicating that preservation does not bias the results toward a deglacial-like pattern. We conclude that the spatial distribution of volcanism is consistent with a deglacially induced increase in volcanism and is unlikely to be an artifact of observational bias.

In an attempt to further quantify the relationship between volcanism and deglaciation, we compare our maps of volcanic frequency against an independent estimate of the degree of deglaciation. While the dimensions of the Laurentide and Feno-Scandian ice sheets are relatively well documented for the Last Glacial Maximum, no corresponding map of the extent of mountain glaciers exists. To obtain a global indication of changes in glaciation, we use estimates of modern accumulation relative to ablation. For accumulation we use the NCEP/NCAR reanalysis of precipitation data (Kalnay et al., 1996), and ablation is calculated using a positive degree approach in combination with daily-average two-meter temperatures, also from reanalysis. In particular, annual ablation is estimated by multiplying 0.15 mm/(day °C) times daily average temperature and summing over all days with a positive ablation. All melt is assumed to run off. Note that some regions have a mass balance that is artificially low because the resolution of the reanalysis smoothes the highest topographic features and spreads out regions of concentrated rainfall. Reassuringly, regions predicted to have the greatest modern mass balance are also those that are presently glaciated (Cogely, 2003) (Fig. 4). These same regions appear, to first order, to have also been more glaciated in the past (Denton and Hughes, 1981; Grosswald, 1998; Dyke, 2004).

To obtain a single index of the relative increase in volcanic frequency during deglaciation, we average together the two separate ratios of deglacial/glacial and deglacial/late-Holocene frequency maps. Prior to averaging, each map is normalized by dividing through by the average ratio at latitudes between 30° North and South, giving each map a similar weighting and facilitating comparison between low- and high-latitude regions. This "normalized eruption frequency" provides an index of the relative increase of volcanism for each

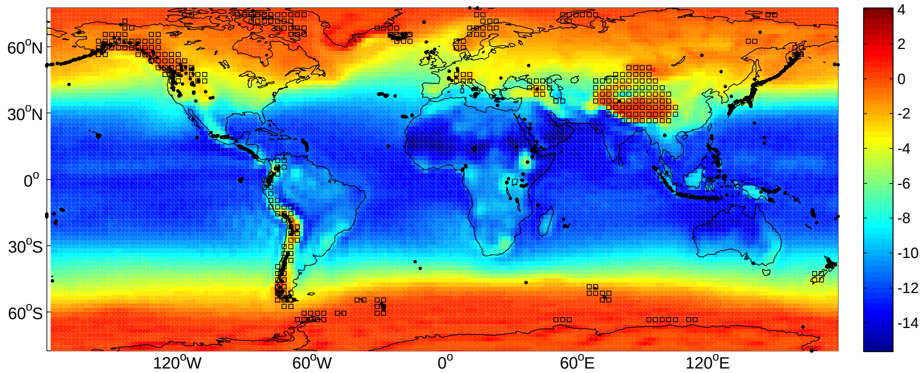

Fig. 4. Modern ice mass balance (m/yr, shading) along with regions containing modern day glaciers (Cogely, 2003) ($3° \times 3°$ black grid boxes). Glacial regions and subaerial volcanos (black dots) are, not coincidentally, often co-located.

region during the deglaciation.

We now have independent and comparable indices of the degree of deglaciation and the eruption frequency during the deglaciation. Fig. 5 shows these indices against one another for each spatial location where a volcano exists. The eruptive index is approximately constant at low values of the deglaciation index, corresponding to regions where no or insignificant deglaciation occurred, but stretches out to values of five or more with higher values of the deglaciation index (Fig. 5). For example, the relative frequency of volcanic events along the Western Pacific Rim increases by more than a factor of five between Indonesia and Kamchatka. The strong function-like relationship between these independent indices supports the hypothesis that deglaciation triggers volcanic activity.

2.2 An estimate of global rates of volcanism

The discussion above documents an increase of global volcanism during the deglaciation. To better interpret these values with regard to the climate sys-

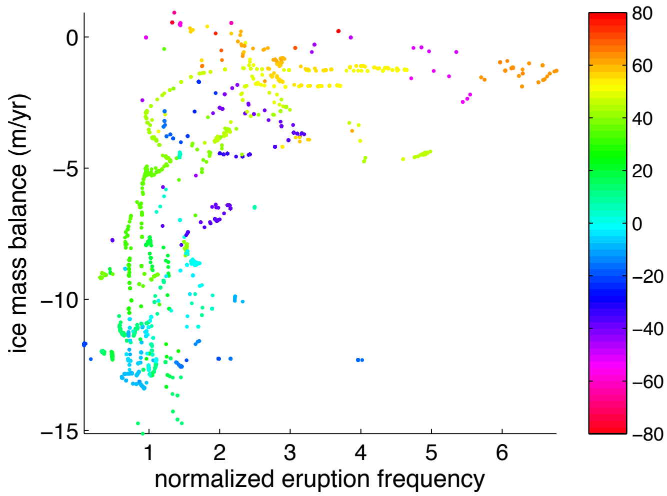

Fig. 5. An index of the eruption frequency during deglaciation plotted against an index of the magnitude of deglaciation (ice-mass balance) for each volcano. Ice mass balance indicates how close a region is in the modern climate to glaciating, and those regions with less-negative mass balance tend to retain some glaciers today (Fig. 4) and to have been more glaciated in the past. Note that mass-balance values tend to be negative both because we are in an interglacial and because the NCEP/NCAR reanalysis does not fully capture the small-scale orographic influences upon temperature and precipitation. The deglacial eruption frequency is once normalized to the glacial eruption frequency (Fig. 3a) and another time to the Holocene eruption frequency (Fig. 3b). These two ratios are then averaged together after normalizing each by their mean values at latitudes between 30° North and South. Records at low-latitude (latitude is indicated by the shading) center around one. Volcanos in regions more prone to glaciation (i.e. those having a less negative mass-balance and, typically, at higher latitudes) are associated with large deglacial eruption frequencies. As the ice-mass balance and eruption frequency are determined independently of one another, their function-like dependence indicates a physical link.

tem, it is useful to quantify the actual magnitude of the increase, not just the relative changes. This requires a method to remove the temporal bias shown in Figure 1. Figure 5 suggests a uniform rate of volcanism in unglaciated regions, and assuming this is the case, it provides a normalization method to remove the temporal bias. In essence, we assume a uniform rate for unglaciated volcanism and use the observations of that data set to determine the temporal bias. We then normalize the data from glaciated regions against those from unglaciated regions in an effort to remove the bias and determine how volcanism varies with time.

We approximate the true frequency of eruptions in unglaciated regions as a constant, $u_\circ$. The observed frequency, u', is always less than $u_\circ$ and the two can be related using an observational bias term, $u'_t = u_\circ b_t$. The bias term, b_t, appears to follow a power-law (Siebert and Simkin, 2002), though our analysis does not depend on its exact form.

For glaciated regions we have $g'_t = g_t b_t$, where the true frequency, g_t, is time dependent. Assuming that the sampling bias is consistent between both groups permits us to use the frequency of unglaciated eruptions as a control by which to estimate the glaciated frequency, $g_t = u_\circ g'_t/u'_t$. Global volcanic frequency is then $v_t = u_\circ(1 + g'_t/u'_t)$, which we present as fractional deviations from the present, $v_t/v_\circ = (1 + g'_t/u'_t)/(1 + g_\circ/u_\circ)$. The critical term in this equation is the ratio of the observed rates of eruptions, g'_t/u'_t, with the other terms acting to scale the results.

The extent to which the observational bias is consistent between the glaciated and unglaciated groups is uncertain, although Figure 6 gives some credence to the point of view that they are similar similar. Of course, evidence of volcanic eruptions in glaciated regions may be disturbed or destroyed by the action of the ice itself. On the other hand, exposure in glaciated regions is often excellent, while unglaciated tropical regions are prone to greater vegetative cover and poor exposure. Also, we are not estimating volumes of eruptions, but eruption frequencies, and it would be rare for glaciation to destroy all evidence of major eruptions, some of which, for example, are dated from far flung ash falls. Another potential difficulty in observational bias is that Western European and North American volcanic systems have been more thoroughly studied, and the historical record in important areas such as Indonesia is poorly known. There is clearly much room for further work in quantifying the global volcanic record.

We divide volcanic events into glaciated and unglaciated groups using the ice mass balance (see Fig. 5). Plausible cut-offs are -9 m/yr (giving an equal frequency of events between the glaciated and unglaciated groups during the last 2 ky) and -6 m/yr (based on where eruptions frequencies shift toward higher values). Either cut-off indicates that the ratio of glaciated to unglaciated eruption frequencies, g'_t/u'_t, is lowest during the last glacial, increases sharply near 12 ka, peaks near 7 ka, and then subsides back toward glacial levels in the recent past (Fig. 6). The -6 m/yr cut-off indicates a doubling of the global frequency of volcanic events between 12-7 ka relative to the last millennium, while -9 m/yr gives a factor of six increase — we expect that the true value is between these bounds. The difference in these ratios may owe to misplacement of glacial and nonglacial volcanos into the opposite category. In future work it would be useful to assess field evidence for deglaciation on a site-by-site basis.

Bryson and co-authors have used earlier versions of their dataset (Bryson et al., 2006) to estimate global rates of volcanism. They assume that the observational bias follows a power-law form (Bryson, 1989) or some other specified distribution (Bryson and Bryson, 1998), and use anomalies from these assumed distributions as indicators of changes in global volcanism. Apart from methodology and use of the updated database (Bryson et al., 2006), the present results also differ from Bryson (1989) and Bryson and Bryson (1998) in that they include many more observations over the last 12 ky (Siebert and Simkin, 2002), show a more distinct increase in volcanism during the deglaciation and subsequent decline during the Holocene, and show little variability during the last glacial. However, all reconstructions agree in showing anomalously large volcanism during the last deglaciation.

It is useful to consider the statistical significance of the increase in global volcanism which we find for the deglaciation. We adopt a null-hypothesis that volcanic systems are uninfluenced by deglaciation. If the null hypothesis holds, the results we obtain for eruption ratios should be consistent with random assignment of volcanos to the unglaciated or glaciated groups. We conducted 10^4 Monte Carlo trials wherein changes in global volcanic activity are computed after randomly assigning volcanic events to the glaciated and unglaciated groups. For the glacial and late Holocene intervals, the results are broadly consistent with the observations, as we would expect. In contrast, for the deglaciation, 99% of the trials have an eruption ratio between 0.5 and 1.5, which is inconsistent with the observation (see Fig. 6b). These results indicate that the factor of two to six increase in volcanic eruptions which we document during the deglaciation is highly significant.

Our estimate of the time-history of global volcanism is also broadly consistent with an independent, albeit more regional, estimate from the Greenland Ice Sheet Project II core which depends on excesses SO_4 concentrations in the ice to identify volcanic events (Zielinksi, 2000). This Greenland record of volcanism indicates that the greatest frequency of volcanic events during the last 40 ky occurred between 15-8 ka and that the largest eruptions occurred between

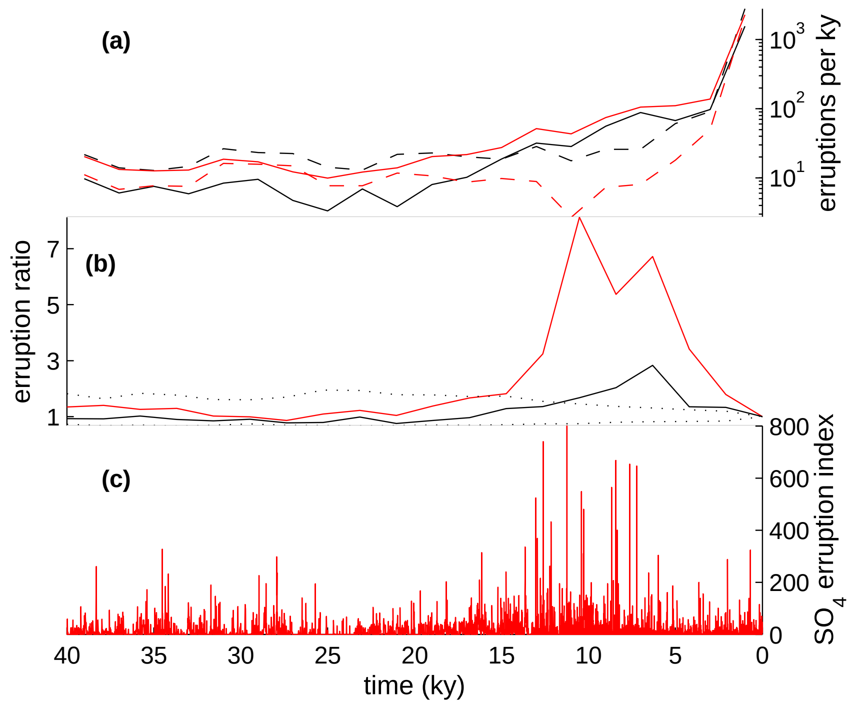

Fig. 6. Changes in volcanic activity over the last 40 ky. **(a)** Number of volcanic events per ky for glaciated (solid line) and unglaciated (dashed) volcanos using a mass-balance cut-off of -6 m/yr (black) and -9 m/yr (red). The -9 m/yr cut-off indicates a larger divergence between the glaciated and unglaciated volcano groups. Note that the y-axis is logarithmic. **(b)** Estimated global volcanic activity using the -6 m/yr (black) and -9 m/yr cut-offs (red). The 99% confidence interval for the null-hypothesis of no systematic difference between glaciated and unglaciated events (dotted lines) indicates that the increase in the eruption ratio during deglaciation is highly significant regardless of which cut-off is used. **(c)** An eruption index based on volcanic SO_4 from a Greenland ice core (Zielinksi, 2000).

13-7 ka, consistent with our reconstruction. Note that the highest concentrations may reflect proximity of the volcanic events and changes in accumulation layer thickness and thus, while indicative, are not directly comparable to the eruption ratio that we calculate. Nonetheless, the correspondence between these independent reconstructions supports the plausibility of both.

Reconstructions of volcanic activity from Antarctica ice cores show conflicting results. A reconstruction of volcanism over the last 40 ky using volcanic SO_4 from Epica Dome C, Antarctica, indicates little change in volcanism (Castellano et al., 2004); whereas an estimate from Siple Dome, based on the optical properties of dust, indicates heightened volcanism near 10 ka (Bay et al., 2004). It is possible that the Antarctic signal reflects the fact that there are far fewer subaerial volcanos at high southern than at high northern latitudes. Siebert and Simkin (2002) identify some 435 volcanos north of 40°N, and only 70 volcanos south of 40°S.

3 Physical mechanisms relating deglaciation and volcanism

The results presented above rely upon inferences drawn from available data, and while indicative, they do not directly get causality. In this section we discuss how the foregoing results are consistent with physical consequences expected from deglaciation.

3.1 Depressurization and melt production

The fraction of melt in the Earth's mantle is sensitive to pressure changes. Experimental data and analysis shows that the amount of melt in the mantle, in regions which are above the solidus, increases by about 1% for each 100 Mpa of pressure decrease (McKenzie, 1984; Langmuir et al., 1992). Thus, for example, unloading one km of ice leads to a ten MPa depressurization and a 0.1% increase in the melt percentage (Jull and Mckenzie, 1996), which is equivalent to 100 m of melt for a melt region 100 km thick. Such a 100 km thickness is consistent with observations of slab thickness at arc volcanic sites (e.g. Syracuse and Abers, 2006), though there is some question regarding how the pressure exerted by surface loading will be distributed at depth. Whereas more detailed modeling of the ice loading and resulting melting at arcs would be useful, we work from the assumption that the pressure increase associated with glacial loading influences the full thickness of the melt column because glacier and ice cap systems during the Last Glacial Maximum were spatially extensive. For example, southern Alaska today retains only isolated mountain glaciers, but during the Last Glacial Maximum it appears to have been covered beneath contiguous ice extending from the Alexander Archipelago in the East to the Aleutian Islands in the West, and extending northward from the Pacific between hundreds to a thousand km (Manley and Kaufman, 2002); the Cascades of northwest North America lay beneath the Western lobe of the Laurentide ice sheet (Dyke, 2004); and southern South America was covered beneath extensive ice fields (Denton and Hughes, 1981).

The volume of mountain glaciers and small ice caps are estimated to have decreased from 1.9 million km^3 during the Last Glacial Maximum to 0.1 million km^3 today (Denton and Hughes, 1981). If only a tenth of this loss of ice volume influences magmatic production (consistent with unloading ice of 200 m thickness from a 50 km swath along 20,000 km of convergent margin), we anticipate 18,000 km^3 of melt production — roughly equivalent to doubling global subaerial volcanism for 5000 years. Or, if a third of the glacier melt is involved, melt production equates to 60,000 km^3, or more than a six-fold increase in subaerial volcanism over 5000 years. These crude estimates are consistent with the upper and lower bounds on deglacial volcanic activity inferred from the observed record of volcanic eruption, indicating that the level of increased volcanism is broadly consistent with the magmatic production expected from the unloading of mountain glaciers and small ice caps. Such a prediction of magmatic emplacements also offers a test of our hypothesis. If a third of the melt volume is erupted, we expect 10 to 20 meters thickness of tephra to be emplaced, on average, in a 50 km swath along 20,000 km of convergent margin, though explosive eruptions and transport of material subsequent to emplacement could lead to a more diffuse distribution.

Mount Mazama is one of the few volcanos which is sufficiently well mapped and dated to permit estimation of the volume of erupted material during deglaciation. Bacon and Lanphere (2006) identify 60 km^3 of material as being erupted at Mount Mazama during the last deglaciation, almost half of the total mapped at that site over the last 400 ky, and corresponding to a roughly 60 m thickness over a 1000 km^2 region. (Bacon and Lanphere, 2006) suggest that several times this mount was emplaced beneath Mount Mazama. Although an isolated study, this work indicates that the eruptive products from one volcano contributed somewhere between 1% and 0.3% of the total melt production we estimate (i.e. $3 \times 60\text{km}^3/18,000\text{km}^3$ to $3 \times 60\text{km}^3/60,000\text{km}^3$). That hundreds of such volcanos are expected to have been active through the deglaciation is then consistent with our global analysis of a large magma output during the last deglaciation. Iceland is also notable, although located on a ridge rather than an arc, in that 3100 km^3 of material are estimated to have been erupted 12 ky ago (Jull and Mckenzie, 1996; Maclennan et al., 2002; Sinton et al., 2005), consistent with the unloading of a two kilometer thick ice cap from the island (Maclennan et al., 2002). This volume alone is equivalent to 1 ky of global output from convergent margin volcanism.

3.2 Glacial pacing of eruptions

As mentioned in the introduction, it appears that subtle variations in loading, flexure, or water content influence the timing of eruptions at monthly to annual timescales (Sparks, 1981; Neuberg, 2000; Mason et al., 2004). If such weak environmental effects influence the timing of an eruption, it also appears likely for the far larger forces associated with glacial loading and unloading to influence when an eruption occurs.

We explore this possibility from the premise that the eruptability of a particular volcano is a balance between the forces generated by melt and gas production within the volcano edifice and the confining pressure and integrity of the surrounding rocks, all of which can be influence by glacial variability. First, melt production was discussed above. Second, removing ice reduces the confining pressure and could trigger an eruption. Third, glacial erosion may cause an ongoing reduction in confining pressure and structural integrity throughout a glacial period. Finally, far field effects, such as from the unloading of the continents and the rising sea level, may encourage volcanism by opening passageways or altering the pressure in magma chambers (Nakada and Yokose, 1992; McGuire et al., 1997).

We focus on the direct effects of changes in ice loading and illustrate this pacing concept using a simple model, similar to that of (Jupp et al., 2004). Magma is modeled as accumulating at a constant rate, r, until a time-variable threshold is surpassed, $r > \tau(t)$, when the volcanic system is assumed to erupt completely and then re-commence accumulation. Jupp et al. (2004) considered the case of a sinusoidal change in the level of the threshold. To adapt this

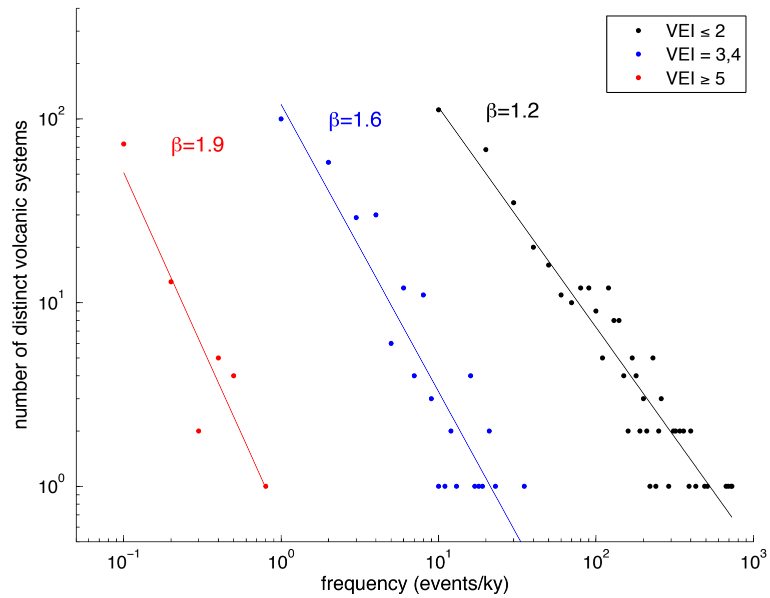

Fig. 7. Histograms of the number of volcanic systems as a function of the average frequency of eruptions. Three separate histograms are shown: one for the VEI one or two events listed in the Volcanoes of the World database over the last century (red), another consisting of eruptions having a Volcanic Explosivity Index (VEI) of three or four over the last millennium (blue), and a final histogram for the VEI$\geq$5 events over the last ten-thousand years (black). It is less likely for eruptions with a large VEI to have been missed back in time (Siebert and Simkin, 2002; Coles and Sparks, 2007), and the groupings are made in an effort to balance the competing objectives of obtaining a long time-series and not missing events. Axes are logarithmic, and the solid lines indicate the slope of a power-law relationship, β, between number of systems and frequency of eruptions. Note that the power-laws become steeper when only higher VEI eruptions are included.

simple accumulation-eruption model to the case of glacial cycles, we parameterized the threshold to depend on variations in ice volume, $\tau = a + bV'(t)$, where the prime denotes that the ice volume variability has been normalized to zero mean and unit variance. A composite benthic δ^{18}O record (Huybers, 2007) is used as a proxy for ice volume. The parameter b controls the strength

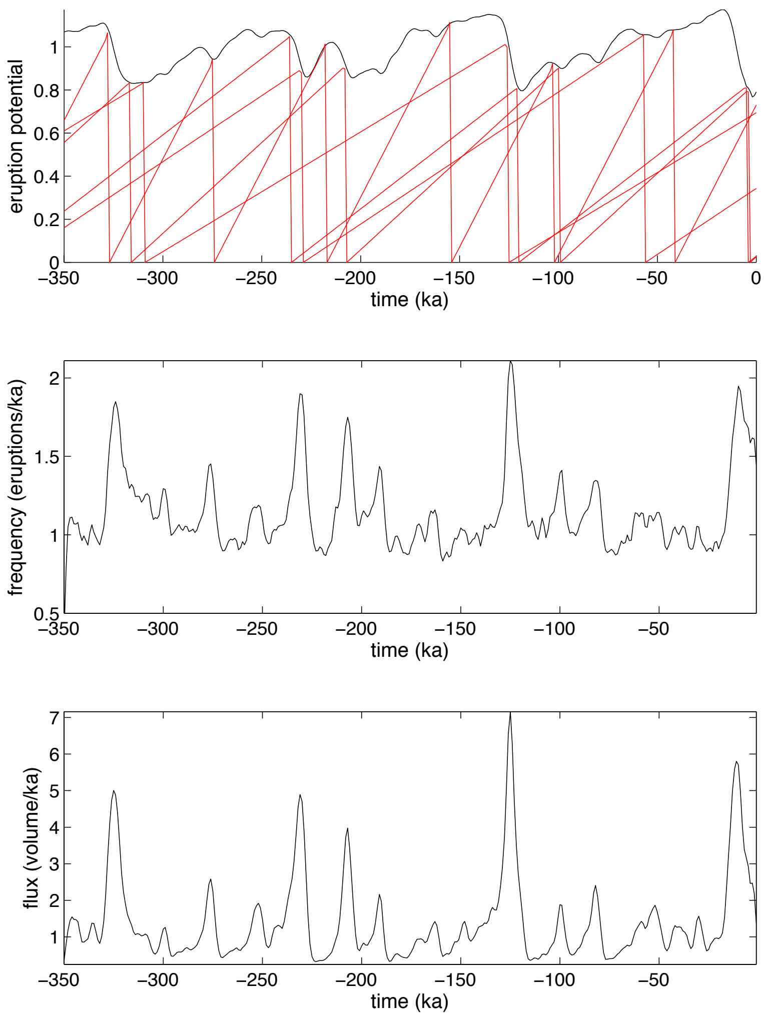

Fig. 8. A toy accumulation-eruption model of the pacing of volcanic eruptions. **(Top)** An eruption threshold is specified with an average value of one and a variance of 0.01 (black line), which follows marine benthic δ^{18}O such that intervals with less ice correspond with a lower threshold for eruption. The model is run 10,000 times and a few representative runs are indicated (red lines). **(Middle)** A histogram of the timing of eruptions derived from an ensemble of runs. For each run the frequency, f, of the volcanic system is drawn from a probability distribution following a power-law with $P \sim f^{-1.9}$, where f ranges between (200 ky)$^{-1}$ to (1 ky)$^{-1}$ (see Fig. 7). **(Bottom)** The flux of tephra is estimated assuming that the volume of an eruption is proportional to the time elapsed since the last eruption. In this scenario, low-frequency volcanic systems are both larger and more likely to be paced by deglaciation, and thus both serve to increase the deglacial volcanic flux. To facilitate interpretation of relative increases, frequencies and rates are normalized to a value of one between 80 and 20 ka.

with which the ice volume variations influence the eruption threshold. The approximate recharge timescale is given by the ratio of a/r, though the exact timing also depends on the structure of the glacial variability.

The longer the recharge timescale, the more likely an eruption is to be paced by the modulation imposed upon the threshold. This follows from the geometrical consideration that shallow accumulation trends are more likely to intersect anomalously low portions of the threshold (see Fig. 8a). Thus, the frequency with which a volcano erupts influences the degree to which glacial cycles pace eruptions in our model. There exists an extensive literature on the elapsed time between volcanic eruptions (e.g. Coles and Sparks, 2007), but we are not aware of any general form for the number of volcanic systems which exhibit a particular eruption frequency, and in estimating such a relationship we are, again, up against the strong bias against observing older eruption. Nonetheless, we seek a rough estimate from the Volcanoes of the World database, using this database because it contains information on the Volcanic Explosivity Index (VEI).

The frequency of eruption of a volcanic system, f, is estimated using the number of observed eruptions occurring within a given time interval. Eruptions sites separated by more than 100 km from one another are considered distinct. The volcanic record appears fairly complete over the last century, and a histogram of eruption frequencies suggests that frequency of individual volcanic systems and the number of such systems, N, can be described by a power-law, $N \sim f^{-\beta}$ (Fig. 7). A least-squares linear fit between $\log_{10}(N)$ and $\log_{10} f$ of all eruptions with a VEI of one or two yields a β of 1.2. (A similar scaling relationship is obtained if all eruptions in the last century are included.) Eruptions with a higher VEI are more likely to be identified back in time, permitting exploration of this power-law behavior at lower frequencies, though at the expense of not including smaller eruptions. Performing a similar log-log fit to the subset of events having a VEI of three or four over the last millennium yields a β of 1.6, and a fit to eruptions having a VEI of five or greater over the last 10,000 years yields a β of 1.9.

The data suggest that larger eruptions follow a steeper scaling relationship, though this could be influenced by observational bias. Regardless, it appears safe to conclude that the power-law is greater than one, implying that systems having a lower eruption frequency are more prevalent and, somewhat counter-intuitively, that more eruptions will result from low than high frequency systems during a given interval. Presumably, this power-law scaling breaks down at certain high and low frequencies, but the suggestion of a quasi-100ky period for the large eruptions documented at Mount Mazama (Bacon and Lanphere, 2006), Western Europe (Nowell et al., 2006) and the South Eastern United Sates (Jellinik et al., 2004), and the even lower-frequency events at Yellowstone (Licciardi and Pierce, 2008) indicates that the power-law relationship may extend beyond the 10 ky period explored here.

The distribution of the size of eruptions also has consequences for potential climate effects. Consider that a VEI one eruption involves between $10^4 - 10^6$ m^3 of tephra, while eruptions having a VEI of $x > 1$ involve $10^{x+4} - 10^{x+5}$ m^3 of tephra. Thus, for example, while the estimates in Fig. 7 indicate that VEI five or greater eruptions are about 10^3 times less frequent as VEI one or two eruptions, they involve 10^5 times more material, and thus dominate budgets of total erupted material. In support of this inference, a second analysis between frequency and VEI (not shown) indicates a scaling relationship well in excess of one.

The indication that large VEI events dominate the volume of erupted material prompts us to parameterize the model in keeping with the results for the VEI$\geq$5 case (Fig. 7). These larger eruptions are also more likely to be consistently identified in the past. We parameterize the recharge timescales, a/r, to follow a power-law distribution with β equal to 1.9 and assume that the power-law distribution holds between frequencies (200 ky)$^{-1}$ to (1 ky)$^{-1}$. We do not observe volcanic eruptions with a VEI greater or equal to five occuring at frequencies higher than (1 ky)$^{-1}$ at any one site, possibly because there is a finite recharge time associated with such large eruptions.

A small value is used for the ice-volume influence upon the threshold of eruptability, $b = 0.1$, relative to a mean threshold of $a = 1$, such that deglaciation has a minor effect on the level of the threshold. Nonetheless, the large number of slow recharge timescale systems provides a high degree of sensitivity to the threshold modulations, and results from a large number of runs indicate a doubling in the number of eruptions during deglaciations (Fig. 8). While obviously simplistic, this model result illustrates how a weak pacing imposed by glacial variability could act to cluster the timing of volcanic eruptions near times of deglaciation, consistent with our observations. Furthermore, the volume of erupted material during deglaciation is expected to undergo greater magnification because low-frequency systems tend to both have larger eruptive volumes and are more likely to be paced by glacial fluctuations. Assuming that the volume of erupted material is proportional to the elapsed time since the last eruptions, there is a factor of five increase in the flux of material during deglaciation (Fig. 8).

To summarize, our simple eruption model suggests a factor of two increase in frequency and a factor of five in volume. Observational analysis of eruption data suggests a factor of two to six increase in volcanism during deglaciation, and the implied increase in melt production in the mantle is consistent with the expected amount of ice unloading. Inclusion of increased melt production during deglaciation, as opposed to only parameterizing a decrease in the eruption threshold, would produce an even more dramatic pacing effect in the model, as might inclusion of glacial erosion or far field unloading effects, but we have not included these additional interactions in our analysis.

4 Implications for the carbon cycle

The data and our model indicate that deglaciation drives a wide-spread increase in volcanism. We hypothesize that elevated volcanism during deglaciation contributes to the rise in atmospheric CO_2 during deglaciation, with the ensuing warming constituting a positive feedback upon the deglaciation. Conversely, waning volcanic activity during the Holocene would contribute to cooling and reglaciation, thus tending to suppress volcanic activity and promote the onset of an ice age. This hypothesis depends on the amount of CO_2 emitted from volcanos, as well as the amount which remains airborne. Thus, in principle, such a calculation depends upon nearly all aspects of the climate system, including parts of the solid earth. Here we seek first-order estimates.

4.1 CO_2 emissions from subaerial volcanos

First, we estimate the subaerial volcanic CO_2 flux. One approach is to multiply arc magma production rates by their average primary CO_2 concentration. Estimates of long term crustal production have been put at 20 to 40 km^3 per km of arc length per million years (Reymer and Schubert, 1984), but this estimate has been criticized as too low by a factor of two (Dimilanta et al., 2002), and both of these estimates are minima with respect to magma additions because they are the net of production after losses due to erosion. A value of 80 km^3/km/Ma and 35,000 km total arc length gives a magma production rate of more than 3 km^3/yr, in accord with other estimates (Dimilanta et al., 2002). Primary CO_2 concentrations cannot be determined directly because CO_2 is almost entirely degassed prior to eruption. Instead, we estimate the concentration of carbon in the mantle by multiplying an average CO_2/Nb ratio of $\sim$500 (Saal et al., 2002; Cartigny et al., 2008) by an average Nb content of $\sim$3 ppm in arc basalts, yielding a 0.15% CO_2 mantle contribution in primary magmas, in agreement with estimates based on modeling the ^{3}He flux from the mantle (Marty and Tolstikhin, 1998; Fischer et al., 1998). Because carbon isotope data and $CO_2/^3He$ ratios both indicate that the mantle contributes only 10-20% of the total CO_2 at arc volcanoes (Marty and Tolstikhin, 1998; Fischer et al., 1998), we arrive at a total estimate of 0.65% to 1.5% CO_2 in primary arc magmas. 1% CO_2 and 3 km^3/yr of magma production leads to a time-average global emission rate of 0.1 Gt/yr, assuming a density of 3 Gt/km^3.

It is harder to parse emissions from non-convergent margin subaerial volcanoes, but they likely add another 0.05 Gt/yr (Marty and Tolstikhin, 1998; Hilton et al., 2002). These estimates are slightly higher than those relying on data from currently active volcanoes (Williams et al., 1992) and estimates derived from $CO_2/^3He$ (Sano and Williams, 1996; Hilton et al., 2002; Marty and Tolstikhin, 1998), which cluster near 0.1 Gt CO_2/yr. But a recent simulation of arc volcanism combined with observational studies (Gorman et al., 2006) suggests that while the range of emissions found in these studies are plausible, the upper end of the range, ~0.14 Gt CO_2/yr, is most likely. We thus estimate modern subaerial volcanic emissions to be between 0.1 to 0.15 Gt CO_2/year.

The relationship between deglacial unloading and emissions of CO_2 is complex and poorly constrained. While depressurization associated with deglaciation is expected to increase the melt fraction, the amount of CO_2 such melt can be expected to mobilize will depend on various factors. If all the CO_2 in the source is already in the silicate melt, then the amount of CO_2 brought to the surface may not depend on changes in the amount of melt at all. On the other hand, if increased melt production at depth also increases melt flux to the surface or if melting taps an increased volume of source region, we would expect greater CO_2 emissions. It is also unclear when and how CO_2 in crustal magma reservoirs reaches the atmosphere. CO_2 solubility is low enough that much of it is released at depth, and this gas might escape at times and locations not directly associated with eruption. The results of Allard et al. (1994) suggest that intrusive emplacement of magma will be associated with significant CO_2 fluxes, but whether such emplacement would occur in response to increasing the melt is uncertain. We also note that eruptions are more directly linked to increased CO_2 emissions and, as noted above, erruption may be paced by glacial variability.

Despite these outstanding questions, we make an estimate of the time history of CO_2 fluxes by multiplying current subaerial volcanic emissions by the ratio between past and present eruption frequencies. This assumes proportional changes between the frequency of volcanic events and CO_2 emissions. Even under these simplifying assumptions, there are multiple uncertain parameters, and we take a probabilistic approach to characterizing the volcanic emissions of CO_2. (Such a probabilistic approach will become increasingly useful for characterizing results because the complexity of the model under consideration increases in later sections.) The time history of volcanic CO_2 emissions is estimated using a random draw from a xuniform distribtution of mass-balance cut-offs (bounded between -6 m/yr and -9 m/yr) and modern fluxes of CO_2 (bounded between 0.1 and 0.15 Gt of CO_2 per year). Repeating this procedure many times provides an ensemble of plausible time-histories of volcanic CO_2 emissions. The ensemble average indicates that volcanoes emitted 3000 Gt of CO_2 during the last deglaciation above a baseline scenario of current emissions, and 90% of all time-histories fall between 1000 to 5000 Gt of CO_2 emissions. These are large numbers. By way of comparison, 3000 Gt of volcanic CO_2 emissions corresponds to roughly a century of anthropogenic emissions at current rates.

4.2 Submarine volcanism

It is also necessary to consider the effects of a rise in sea level following from the unloading of ice from the continents, which will tend to decrease ridge volcanism. Because water is roughly a third the density of the mantle, the 135 m deglacial rise in sea level is equivalent to suppressing 45 m of mantle ascent beneath an ocean ridge. Given an average mantle upwelling rate of $\sim$3 cm/yr at ridges, this is equivalent to suppressing $\sim$1.5 ky of melt. Measurements of $CO_2/^3He$ and CO_2/Nb ratios from ridge system indicate that total emissions are $\sim$0.1 Gt/yr (Marty and Tolstikhin, 1998; Saal et al., 2002; Cartigny et al., 2008). 1.5 ky of lost emissions then equates to $\sim$150 Gt CO_2, or more than an order of magnitude less than the estimated increase in arc CO_2 emissions.

Ridges have a minor influence on carbon emissions because they are depleted in CO_2 by a factor of 5 to 10 relative to emissions at arc volcanoes (Marty and Tolstikhin, 1998; Fischer et al., 1998; Saal et al., 2002; Cartigny et al., 2008) and the greater rates of ridge production lead to smaller fractional changes in production from loading. Thus, the suppression of ridge volcanism by rising sea-level appears to have little consequence for ocean-atmosphere carbon values. There also exists the possibility that rising sea level would suppress volcanic activity on islands (McGuire et al., 1997), but recalculation of global eruption rates excluding island volcanoes indicates no systematic pattern and yields similar rates of global volcanism.

If the glacial/interglacial variations in sea level lead to modulations in the production of melt at mid-ocean ridges, a signature of these variations might be preserved in the bathymetry surrounding spreading centers. Quasi-periodic variability in the sea-floor elevation on length scales of kilometers have been documented, and given spreading rates on the order of one to ten cm per year, the variability is plausibly consistent with the timescales of the glacial cycles. However, our analysis of many sections of high-resolution bathymetry (Carbotte et al., 2004) indicate that the spectra associated with this topography and its correlation with estimates of past changes in sea-level is consistent with that expected from chance alone. Our inability to detect a glacial/interglacial signature in the sea floor bathymetry suggests that other processes, such as those associated with thermal subsidence, dominate the variability (e.g Malinverno, 1991). We hypothesize, however, that detailed time series of ridge bathymetry might reveal an imprint of glacial-interglacial variations in sea level once sufficient data are available.

4.3 Ocean carbonate compensation

A 1000 to 5000 Gt CO_2 release from subaerial volcanoes is expected to increase ocean acidity and, absent other effects, lead to a shoaling of the oceanic carbonate saturation horizon, but such a flux must be considered in conjunction with other influences upon the carbon system. We begin with a simple example that neglects organic land carbon storage and marine carbonate compensation. Assuming that subaerial volcanoes inject ~3000 Gt of CO_2 into the ocean, and also accounting for a 4°C ocean warming (Schrag et al., 1996) and 100 ppm increase in atmospheric CO_2 concentration coming out of the last glacial, we then expect the carbonate saturation horizon to shoal by about 1 km (Fig. 9). Such a shoaling is consistent with observations of carbonate dissolution in the Pacific (Farrell and Prell, 1989; Thunell et al., 1992) but not the Atlantic (Thunell et al., 1992). Note that we compute the change in the saturation horizon only accounting for the influence of pressure upon dissolution, and not the more uncertain and less important vertical gradients in temperature or salinity.

It is also necessary to consider the ~0.3‰ increase in ocean $\delta^{13}C$ observed between the glacial and Holocene (Curry et al., 1988), which is normally interpreted as indicating a biospheric uptake of ~1500 Gt of CO_2. A further ~500 Gt CO_2 of organic uptake is needed to compensate for volcanic carbon emission having an isotopic ratio of -3.8 ± 1.2‰(Sano and Marty, 1995; de Leeuw et al., 2007), still assuming 3000 Gt CO_2 of volcanic emissions. The net carbon in the ocean/atmosphere system then increases by only 1000 Gt of CO_2, and when this is taken together with the mean ocean warming, the expected change in the carbonate saturation horizon is indistinguishable from zero (Fig. 9), particularly given further uncertainties associated with the carbonate system such as coral reef building (Vecsei and Berger, 2004). Such a small change in saturization is also consistent with estimates of carbonate ion concentration during the last glacial (Broecker and Clark, 2001; Anderson and Archer, 2002), which suggest changes in the distribution of water masses, but little change in overall concentration. We also note that the additional flux of CO_2 from volcanoes is consistent with inferences that no one oceanic mechanism is capable of explaining the glacial/inter-glacial changes in atmospheric CO_2 (e.g. Kohfeld et al., 2005; Marchitto et al., 2005).

In future studies it may be useful to calculate the expected influence of volcanic carbon emission on the carbonate system under various, assumed scenarios, but here we proceed most simply, assuming that the changes in saturation horizon are negligible. Under this assumption, carbonate compensation plays no significant role in determination of the atmospheric CO_2 concentration coming out of the last glacial, and we do not include this process in our consideration of the equilibration of carbon between the atmosphere and ocean during the last deglaciation.

4.4 A simple time-variable model of atmospheric CO_2

A simple two-box model, similar to that of (Kheshgi, 2004), is adopted to represent the time-variable volcanic influence upon atmospheric CO_2,

$$\begin{aligned} \mathrm{d}a/\mathrm{d}t &= -F_t + V_t - W_\circ, \\ \mathrm{d}b/\mathrm{d}t &= F_t. \end{aligned} \tag{1}$$

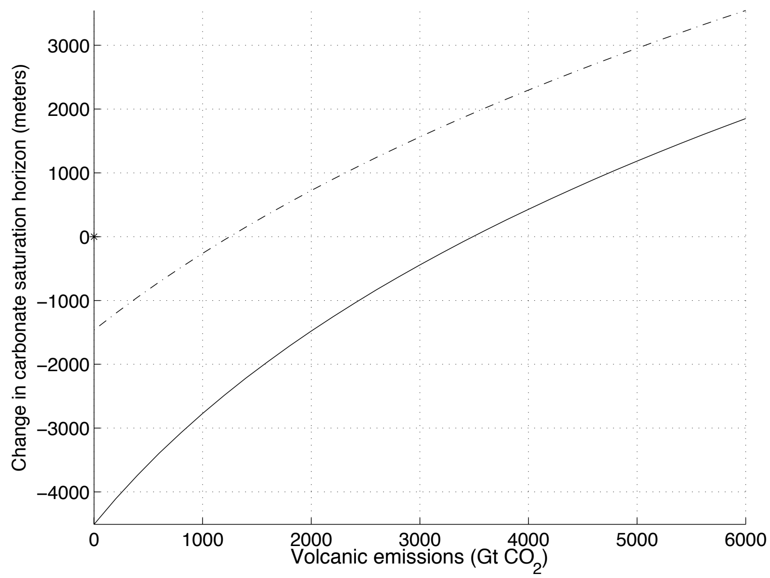

Fig. 9. Modeled change in the carbonate saturation horizon coming out of the last glacial for various volcanic inputs of CO_2 into the ocean atmosphere system. One scenario considers the case without changes in organic storage of carbon on the continents (dashed line) and the other with organic storage (solid line).

Here a and b are the amounts of inorganic carbon in the atmosphere and ocean, measured in Gt of CO_2. The atmosphere-ocean flux is $F = (a' - b'(1-q)/q)/\tau$, where the primes indicate anomalies away from equilibrium. q represent the fraction of volcanic carbon remaining in the atmosphere once in equilibrium with the ocean, and is taken to be between 10% and 15% (Montenegro et al., 2007). Estimates of τ range from $\sim$300 years (Archer, 2005) to $\sim$1800 years (Montenegro et al., 2007) or longer (Wunsch and Heimbach, 2008), and we assign wide bounds on τ of 300 ys to 2000 ys. V is the volcanic flux of carbon into the atmosphere, and it is assumed to be in balance with uptake by a constant silicate weathering, $W_\circ$, over the course of a 100 ky glacial cycle. The average CO_2 emissions between 40-20 ka are assumed to equal the unmonitored rates between 100-40 ka. Note that while this model is simplistic, it is able to reproduce the major features in the variability of atmospheric CO_2 found in more complete atmosphere-ocean carbon models (Kheshgi, 2004; Archer, 2005). Furthermore, the results presented here are consistent with those obtained by forcing a more sophisticated carbon box model that has a representation of ocean carbonate compensation and the biosphere (Joos et al., 1996, 2004) (F. Joos personal communication).

To explore the range of atmospheric CO_2 scenarios consistent with our estimates, we again use an ensemble of model results. Parameters are drawn from uniform distributions between the previously discussed bounds: -9 to -6 m/yr for the cut-off used to distinguish glacial and non-glacial volcanos, 0.1 to 0.15 Gt CO_2/yr for the modern volcanic flux, 300 to 2000 ys for the ocean equilibration time, and 10% to 15% for the airborne CO_2 fraction. We take the mean of an ensemble of 10^4 runs as the best estimate and report the associated 90% confidence interval. Each run is initialized at 40 ka with the atmosphere and ocean in equilibrium. The time history of atmospheric CO_2 expressed in the ensemble of model runs can then be compared against atmospheric CO_2 observations obtained from the Dome C (Monnin et al., 2001) and Taylor Dome (Indermühle et al., 2000) ice cores. We consider four distinct intervals (Fig. 10):

(1.) During the glacial, between 40 to 18 ka, model results indicate atmospheric CO_2 decreases by 10 ppm (5 to 20 ppm, 90% confidence interval), marginally consistent with the observed 20 ppm decrease, suggesting that the trend toward lower atmospheric CO_2 levels during glaciation is partly attributable to excess weathering relative to volcanic emissions. (2.) The first half of the deglaciation (18 to 13 ka) contains a modest $\sim$10 ppm (5 to 40 ppm, 90% c.i.) volcanogenic CO_2 increase, whereas observations show a 50 ppm rise, highlighting the fact that factors independent of volcanism exert influence on

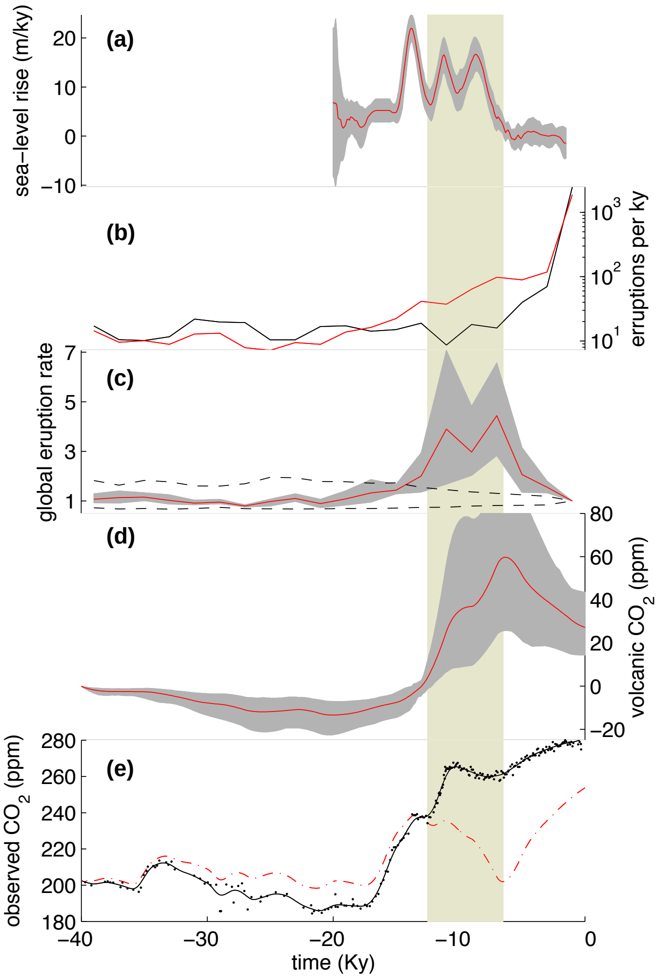

Fig. 10. The last deglaciation. **(a)** Rate of change in sea level estimated from coral records (Fairbanks and Peltier, 2006) along with a Monte Carlo derived estimate of the 90% confidence interval, accounting for the uncertainty, among others, in the depth habitat of the corals (gray shading). **(b)** Number of volcanic events per ky for glaciated (red) and unglaciated (black) volcanos, where the y-axis is logarithmic. **(c)** Estimated global volcanic activity (both glaciated and unglaciated, red line) and the 99% confidence interval for the null-hypothesis of no systematic difference between glaciated and unglaciated events (dashed lines). **(d)** The contribution to atmospheric CO_2 from volcanic activity (red line). Quantities indicated by solid lines (b,c, and d) and gray shading (c and d) are the averages and 90% confidence intervals derived from a 10,000 member ensemble of model runs. Displays in b and c are similar to Fig. 6 but now using the ensemble results. **(e)** CO_2 concentrations from Dome C (Monnin et al., 2001) and Taylor Dome (Indermühle et al., 2000), placed on a consistent timescale (Monnin et al., 2004) (black dots), and a smoothed version using a 2 ky window (black line). Also shown is the residual atmospheric CO_2 after removal of the volcanic contribution (red dash-dot line). The vertical shaded bar indicates the time period between 12-7 ka, when volcanic frequency appears the greatest.

glacial-interglacial variations in CO_2 (Broecker and Peng, 1982). (3.) The second half of the deglaciation (13 ka to 7 ka), however, contains a 40 ppm (15 to 70 ppm, 90% c.i.) increase in volcanogenic CO_2, consistent with observation, particularly with respect to the sharp uptick near 12 ka. This late volcanic contribution is also consistent with its acting as a feedback upon deglaciation, a point we return to later. (4.) In the late Holocene, after 7 ka, volcanic CO_2 contributions wane owing to lower volcanic activity and on-going equilibration with the oceans and weathering, while observations instead indicate rising CO_2 levels during this interval. (It appears that this divergence between the modeled volcanogenic CO_2 and observations is peculiar to the Holocene, as opposed to prior interglacials, a point which we will take up elsewhere.)

This analysis suggests that the excess volcanic emission of CO_2 coming out of the last glacial contributes roughly half of the deglacial increase in atmospheric CO_2. While there are significant remaining uncertainties associated with such a conclusion, it appears that this coupling between the deep earth potentially plays an important role in the determination of glacial/interglacial changes in climate.

4.5 Atmospheric carbon isotopes

As a final line of inquiry, the volcanogenic emissions of CO_2 will be radioactively inert, and thus have some implications for atmospheric radiocarbon activity. The average rate of decline in atmospheric $\Delta^{14}C$ over the last 40 ka, as indicated by the estimates of Hughen et al. (2004), is $-15‰$/ka. During the last deglaciation, 18-7 ka, this rate of decrease appears more than twice as fast ($-33‰$/ka), and Broecker and Barker (2007) have called particular attention to the rapid decline in the subinterval between 17.5-14.5 ka, $-70‰$/ka, the source of which remains unknown. Our estimates place the bulk of the volcanic emissions later in the deglaciation, overlapping with a yet more rapid drop in atmospheric $\Delta^{14}C$ between 12.5 and 10 ka, $-90‰$/ka, which is intriguing. But in the idealized circumstance of 3000 Gt of volcanic CO_2 and instantaneous mixing between the atmosphere and ocean, the atmospheric radiocarbon activity is expected to decrease by only $\sim 20‰$. While the transient atmosphere and surface ocean radiocarbon anomalies may be larger, it seems inescapable that these levels of volcanic emissions are but a minor influence upon the time-history of atmospheric radiocarbon values. Similarly, the expected change in atmospheric $\delta^{13}C$ from volcanic emsissions is trivial relative to the observed variability (Smith et al., 1999).

5 Discussion and speculation

The foregoing results indicate a feedback between glacial cycles and subaerial volcanism. There exists both observational and theoretical support for the concept that deglacial unloading promotes a wide-spread increase in volcanic activity, though such a conclusion would be strengthened through use of more complete catalogs of past volcanic eruption and further detailed studies of the timing of volcanism at individual sites. The increase in volcanic activity leads to a rise in atmospheric CO_2 concentration, which with the implied surface warming, constitutes a positive feedback on deglaciation. Such a feedback between glaciation and volcanism suggests that deglaciation would not only pace eruptions but possibly also be paced by eruptions. That is, the conditions exist for volcanic eruptions and glacial cycles to mutually influence one another's timing so as to become synchronized (Strogatz, 1994). It may be that the progression of Pleistocene climate toward larger and more asymmetric glacial cycles (Huybers, 2007) can, in part, be understood as the synchronization and attendant amplification of the feedback between volcanic systems and glacial variability.

That said, the actual climatic consequences of increased volcanic activity remain uncertain on several counts. The relationship between total magma production rates and the rate of CO_2 emissions is poorly understood, in part because primary CO_2 contents at convergent and divergent margin magmas are poorly constrained. Furthermore, the pathways by which CO_2 escapes from volcanic systems into the atmosphere are not well characterized. Much of the CO_2 appears to volatilize at depth during magma ascent and be added passively to the atmosphere, as opposed to emission through eruptions (Allard et al., 1994). Our analysis has also not considered changes in rates of weathering, even though these are also expected to respond to variations in climate, and may also increase in response to fresh basalt following emplacement during the deglaciation. Finally, the rate of equilibration and partition of emitted CO_2 between the atmosphere, ocean, biosphere, sediments, and solid earth remains a challenging problem.

It is also intriguing that the large uptick in volcanic appears at 12 ka, whereas the deglacial rise in sea-level commenced near 18 ka (Fig. 6). There are several possible explanations for this lag of volcanism behind deglaciation. We first note that a similar delay in the increase in volcanic activity is observed in the Greenland ice core record (Zielinksi, 2000), suggesting that the explanation is physical, as opposed to an observational artifact. It appears most likely to us that the initial deglaciation involved melt from the eastern Laurentide and

Antarctic ice sheet which did not much influence volcanism. In contrast, the highly active volcanic regions covered by the western Laurentide appear to have become more glaciated near 18 ka, and then not to have undergone significant deglaciation until 12 ka (Dyke, 2004). Likewise, the volcanic regions in Alaska (Yu et al., 2008) and Iceland (Maclennan et al., 2002; Licciardi et al., 2007) experienced the most pronounced deglaciation near 12 ka. South American deglaciation is less well constrained, but appears to have proceeded in a series of steps between 17 and 11 ka (McCulloch et al., 2000). Overall, the discrepancy in timing between the initial rise in sea-level and increased volcanism reflects the differing regional histories of deglaciation. One question which then arises is why did the Bölling/Alleröd warming documented at Greenland and many other northern sites not lead to significant retreat of ice caps and glaciers in Alaska, Iceland, or elsewhere? One answer is that Bölling/Alleröd warming was primarily a winter warming associated with decreased winter sea ice (e.g. Denton et al., 2005). Warmer winters and less sea ice would be expected to increase moisture availability and snowfall and, thus, may actually cause ice caps and glaciers to grow.

Other, non-exclusive possibilities for the offset between the beginning of the deglaciation and the increase in volcanism include that tephra from eruptions early in the deglaciation were poorly preserved or that some other observational bias exists. Alternatively, there could exist a time lag between depressurization and eruption, perhaps of several ky. The pacing mechanism provides yet another explanation for the volcanic pulse in the second half of the deglacial. An idealized study of the pacing of eruptions by a periodic modulation of a threshold (Jupp et al., 2004) indicates that eruptions tend to cluster near the minimum in the threshold for an eruption, which in the present case would suggest a clustering of eruptions near the tail end of the deglaciation. Volcanoes are more likely to erupt only once a substantial portion of the load has been removed, as can also be seen in the results presented in Fig. 8. That the uptick in volcanism apparently lags behind both the deglaciation and the initial rise in atmosphere CO_2 also serves to highlight that the volcanic tapping of mantle CO_2 is a feedback upon deglaciation and that other reservoirs of CO_2, notably the ocean (Broecker and Peng, 1982), remain likely contirbutors to glacial/interglacial variations in atmospheric CO_2 .

Co-variability between CO_2 and proxies of air temperature in Anarctica have been interpreted as evidence for Southern Ocean control over atmospheric CO_2 concentrations (Monnin et al., 2001), and which might be construed to preclude partial control of CO_2 by volcanic emission. Our view is that temperatures in Antarctica, and the Southern Hemisphere in general, are more likely to be merely in equilibrium with atmospheric CO_2 concentrations. Indeed, surface ocean temperatures and other climate indicators in the Southern Hemisphere also closely covary with CO_2 (Barrows et al., 2007). Perhaps the Southern Hemisphere remains nearly in equilibrium with atmospheric CO_2 concentrations through the last deglaciation, unlike the Northern Hemisphere, because there were no large changes in the distribution of southern continental ice volume (e.g. Huybers and Denton, 2008). Such a view point is supported by a model simulation which has reproduced Antarctic warming through the last deglacation by prescribing atmospheric CO_2 values, along with smaller contributions from changes in ice sheet elevation and Earth's orbital configuration (Timmermann et al., in press), without need to specify the source of that CO_2.

A question also exists regarding the relative importance of the competing volcanic influences on climate associated with atmospheric aerosol loading and CO_2 emissions. Consider the case of the Mount Pinatubo eruption in 1991. It injected about 17 Mt of SO_2 into the atmosphere and had a peak radiative cooling effect of $4 W/m^2$ at the surface, causing surface temperatures to cool by about 0.5°C (Hansen et al., 1992), and diminished with an e-folding timescale of approximately one year. By comparison, we estimate volcanism contributes $\sim$40 ppm to the early interglacial atmosphere, causing an increase in radiative forcing of $\sim$1 W/m^2. In this rough view, volcanic CO_2 forcing is equal in magnitude but opposite in sign to the aerosol effect of a Mount-Pinatubo-like eruption every four years. The competing influences of volcanic CO_2 and aerosol emissions is like the case of the tortoise and the hare: a persistent flux of CO_2 combined with a long atmospheric residence make volcanic CO_2 emissions a powerful climate driver at long time scales. Note that both cooling and warming effects may have had significance for the last deglaciation. Indeed, the large increase in volcanism near 12 ka presumably increased aerosol loading and may be related to the regional, short-term resumption of glacial-like conditions associated with the Younger Dryas, though a recent detailed study of the timing of volcanism in Iceland supports a chronology wherein the bulk of Icelandic eruptions post-date the Younger Dryas (Licciardi et al., 2007).

As a final point, we consider the general conditions which would give rise to the glacio-volcano-CO_2 feedback outlined here. One neccessary condition is for ice and volcanoes to be in proximity (e.g. Fig. 4). At a basic level, a volcanos' orography tends to promote preciptiation and their elevation helps to retain that precipitation as ice. Furthermore, the current plate configuration may be peculiarly conducive to generating glaciated volcanoes, as it places many at high latitudes and along the western margins of continents, which are thus well-situated to capture precipitation from moisture-laden westerlies. A second condition for evoking the glacio-volcano-CO_2 feedback is sensitivity of glacier mass to changes in atmospheric CO_2. Thus, for example, limited ice volume during the Paleocene and Eocene would limit the feedback. Futhermore, climates with high CO_2 will have a lower sensitivity to a given magnitude of volcanic CO_2 emissions because radiative forcing scales nearly logarithmically with CO_2 concentration. Turning to a constrasting environment, the massive ice unloading postulated to occur at the termination of a snowball Earth episode would presumably lead to a dramatic increase in volcanism (Hoffman et al., 1998), though the high atmospheric CO_2 conditions thought to accompany such a deglaciation would again serve to minimize the climate effects associated with volcanic CO_2 emissions. (Volcanism may, however, play a role in the termination of a snowball through wide spread deposition of tephra leading to a decrease in ice albedo.) It thus seems that conditions during the Pleistocene — wherein the Earth has been precariously poised between glaciated and unglaciated states, atmospheric CO_2 concentrations have been modest, and the plate configuration places volcanoes in cold and wet climates — makes this epoch unusually well-suited to evoking the glacio-volcano-CO_2 feedback.

In conclusion, a balance is expected between emissions of CO_2 from volcanoes and uptake by weathering at million year time scales (Walker et al., 1981). At shorter timescales, however, we suggest that deglacially induced anomalies in volcanic activity cause imbalances in the atmospheric carbon budget which accumulate through deglaciations and persist into interglacials. Factor of two to six increases in the rate of volcanic emissions, persisting for thousands of years, are estimated to increase atmospheric CO_2 concentrations by 20 to 80 ppm. While multiple other mechanisms almost certainly contribute to glacial/interglacial CO_2 variability, this increase in volcanism is expected from the effects of deglacial unloading and coincides with the observed secondary deglacial rise of atmospheric CO_2. Thus, the deglacial rise in atmospheric CO_2 can, in part, be understood as a feedback induced by the deglaciation itself and mediated by volcanic activity. By similar logic, the glacial drawdown in CO_2 may partly owe to a deficit in volcanic emissions relative to CO_2 drawdown by weathering and other processes. All this suggests that the Earth system is deeply coupled. So long as the climate and continental configuration engender co-location of volcanoes and ice, we expect interactions between the Earth's interior, surface, and atmosphere to amplify and modify the cycling between glacial and interglacial climates.

Acknowledgments

R. Alley, W. Broecker, M. Dungan, J. Higgins, P. Molnar, T. Plank, D. Schrag, S. Sparks, and P. Wallace provided useful feedback on this work. We would also like to thank M. Cook, J. Higgins, P. Koehler, F. Joos, D. Schrag, and D. Sigman for discussion regarding changes in atmospheric CO_2 concentrations and carbon isotope ratios, and L. Siebert for making an updated version of the Volcanoes of the World dataset available to us.

References

Allard, P., Carbonnelle, J., Metrich, N., Loyer, H., Zettwoog, P., 1994. Sulphur output and magma degassing budget of Stromboli volcano. Nature 368 (6469), 326–330.

Anderson, D., Archer, D., 2002. Glacial-interglacial stability of ocean pH inferred from foraminifer dissolution rates. Nature 416 (6876), 70–73.

Archer, D., 2005. Fate of fossil fuel CO2 in geologic time. J. of Geophys. Res. 110(C09S05).

Bacon, C., Lanphere, M., 2006. Eruptive history and geochronology of Mount Mazama and the Crater Lake region, Oregon. GSA Bulletin 118(11-12), 1331–1359.

Barrows, T., Juggins, S., De Deckker, P., Calvo, E., Pelejero, C., 2007. Long-term sea surface temperature and climate change in the Australian–New Zealand region. Paleoceanography 22 (2).

Bay, R., Bramall, N., Price, P., 2004. Bipolar correlation of volcanism with millennial climate change. Proceedings of the National Academy of Sciences 101 (17), 6341–6345.

Best, J., 1992. Sedimentology and event timing of a catastrophic volcaniclastic mass-flow, Volcan Hudson, southern Chile. Bull. Volcanol. 54, 299–318.

Bigg, G., Clark, C., Hughes, A., 2008. A last glacial ice sheet on the Pacific Russian coast and catastrophic change arising from coupled ice–volcanic interaction. Earth and Planetary Science Letters 265, 559–570.

Boulton, G., Dongelmans, P., Punkari, M., Broadgate, M., 2001. Palaeoglaciology of an ice sheet through a glacial cycle: the European ice sheet through the Weichselian. Quaternary Science Reviews 20 (4), 591–625.

Broecker, W., Barker, S., 2007. A 190‰drop in atmosphere's Δ14C during the Mystery Interval(17.5 to 14.5 kyr). Earth and Planetary Science Letters 256 (1-2), 90–99.

Broecker, W., Clark, E., 2001. Glacial-to-Holocene Redistribution of Carbonate Ion in the Deep Sea. Science 294 (5549), 2152–2155.

Broecker, W. S., Peng, T. H., 1982. Tracers in the sea. Lamont-Doherty Earth

Observatory of Columbia University.

Bryson, R. A., 1989. Late Quaternary Volcanic Modulation of Milankovitch Climate Forcing. Theoretical and Applied Climatology 39, 115–125.

Bryson, R. U., Bryson, R. A., 1998. Application of a Global Volcanicity Time-Series on High-Resolution Paleoclimatic Modeling of the Eastern Mediterranean. Water, Environment and Society in Times of Climatic Change: Contributions from an International Workshop Within the Framework of International Hydrological Program (IHP) UNESCO, Held at Ben-Gurion University, Sede Boker, Israel from 7-12 July 1996.

Bryson, R. U., Bryson, R. A., Ruter, A., 2006. A calibrated radiocarbon database of late Quaternary volcanic eruptions. eEarth Discuss 1, 123–134.

Carbotte, S., Arko, R., Chayes, D., Haxby, W., Lehnert, K., OHara, S., Ryan, W., Weissel, R., Shipley, T., Gahagan, L., et al., 2004. New integrated data management system for Ridge 2000 and MARGINS research. EOS Trans. AGU 85.

Cartigny, P., Pineau, F., Aubaud, C., Javoy, M., 2008. Towards a consistent mantle carbon flux estimate: Insights from volatile systematics (H2O/Ce, δD, CO2/Nb) in the North Atlantic mantle (14 N and 34 N). Earth and Planetary Science Letters 265, 672–685.

Castellano, E., Becagli, S., Jouzel, J., Migliori, A., Severi, M., Steffensen, J., Traversi, R., Udisti, R., 2004. Volcanic eruption frequency over the last 45 ky as recorded in Epica-Dome C ice core (East Antarctica) and its relationship with climatic changes. Global and Planetary Change 42 (1-4), 195–205.

Cogely, J. G., 2003. Global hydrographic data, release 2.3.

Coles, S., Sparks, R., 2007. Extreme value methods for modeling historical series of large volcanic magnitudes. In: Mader, H., Coles, S., Connor, C., Connor, L. (Eds.), Statistics in Volcanology. Vol. 1. Geological Society London on behalf of IAVCEI, pp. 47–56.

Curry, W. B., Duplessy, J.-C., Labeyrie, L. D., Shackleton, N. J., 1988. Changes in the distribution of δ^{13}C of deepwater ΣCO_2 between the last glaciation and the Holocene. Paleoceanography 3, 317–341.

de Leeuw, G., Hilton, D., Fischer, T., Walker, J., 2007. The He–CO2 isotope and relative abundance characteristics of geothermal fluids in El Salvador and Honduras: New constraints on volatile mass balance of the Central American Volcanic Arc. Earth and Planetary Science Letters 258 (1-2), 132–146.

Denton, G., Alley, R., Comer, G., Broecker, W., 2005. The role of seasonality in abrupt climate change. Quaternary Science Reviews 24 (10-11), 1159–1182.

Denton, G., Hughes, T., 1981. The Last Great Ice Sheets. Wiley-Interscience.

Dimilanta, C., Taira, A., Tokuyama, H., Yumul, G., Mochizuki, K., 2002. New rates of western Pacific island arc magmatism from seismic and gravity data. Earth and Planetary Science Letters 202, 105–115.

Dyke, S., 2004. An outline of North American deglaciation with emphasis on central and northern Canada. In: Quaternary Glaciations: Extent and Chronology. Elsevier, pp. 373–424.

Dzurisin, D., 1980. Influence of fortnightly earth tides at Kilauea volcano, Hawaii. Geophys. Res. Lett. 7, 925–928.

Fairbanks, R., Peltier, W., 2006. Global glacial ice volume and Last Glacial Maximum duration from an extended Barbados sea level record. Quaternary Science Reviews 25, 3322–3337.

Farrell, J., Prell, W., 1989. Climatic change and CaCO3 preservation: An 800,000 year bathymetric reconstruction from the central equatorial Pacific

Ocean. Paleoceanography 4 (4), 447–466.

Fischer, T., Giggenbach, W., Sano, Y., Williams, S., 1998. Fluxes and sources of volatiles discharged from Kudryavy, a subduction zone volcano, Kurile Islands. Earth and Planetary Science Letters 160 (1-2), 81–96.

Gardeweg, M., Sparks, R., Matthews, S., 1998. Evolution of Lascar volcano, northern Chile. J. Geol. Soc. Lond. 155, 89–104.

Gorman, P., Kerrick, D., Connolly, J., 2006. Modeling open system metamorphic decarbonation of subducting slabs. Geochem. Geophys. Geosyst 7.

Grosswald, M., 1998. Late-Weichselian ice sheets in Arctic and Pacific Siberia. Quaternary International 45–46, 3–18.

Hall, K., 1982. Rapid deglaciation as an initiator of volcanic activity: An hypothesis. Earth Surf. Processes Landforms 206 (7), 45–51.

Hamilton, W., 1973. Tidal cycles of volcanic eruptions: Fortnightly to 19 yearly periods. J. Geophys. Res. 78, 3363–3375.

Hansen, J., Lacis, A., Ruedy, R., Sato, M., 1992. Potential climate impact of Mount Pinatubo eruption. Geophysical Research Letters 19, 215–218.

Hilton, D., Fischer, T., Marty, B., 2002. Nobel gases and volatile recycling at subduction zones. In: Porcelli, D., Ballentine, C., Wieler, R. (Eds.), Noble Gases in Geochemistry and Cosmochemistry. Vol. 47. Review in Mineralogy and Geochemistry, pp. 319–370.

Hoffman, P., Kaufman, A., Halverson, G., Schrag, D., 1998. A Neoproterozoic Snowball Earth. Science 281 (5381), 1342–1346.

Hughen, K., Lehman, S., Southon, J., Overpeck, J., Marchal, O., Herring, C., Turnbull, J., 2004. ^{14}C activity and global carbon cycle changes over the past 50,000 years. Science 303, 202–207.

Huybers, P., 2007. Glacial variability over the last two million years: an extended depth-derived agemodel, continuous obliquity pacing, and the Pleistocene progression. Quat. Sci. Rev. 26, 37–55.

Huybers, P., Denton, G., 2008. Interpolar climate symmetry at orbital time scales and the duration of Southern Hemisphere summer. Nature Geoscience 1, 787–792.

Indermühle, A., Monnin, E., Stauffer, B., Stocker, T., Wahlen, M., 2000. Atmospheric CO_2 concentration from 60 to 20 kyr BP from the Taylor Dome ice core, Antarctica. Geophys. Res. Lett 27 (5), 735–738.

Jellinik, A., Manga, M., Saar, M., 2004. Did melting glaciers cause volcanic eruptions in eastern California? Probing the mechanics of dike formation. J. of Geophys. Res. 109.

Johntson, M., Mauk, F., 1972. Earth tides and the triggering of eruptions from Mount Stromboli. Nature 239, 266–267.

Joos, F., Bruno, M., Fink, R., Siegenthaler, U., Stocker, T., Le Quere, C., Sarmiento, J., 1996. An efficient and accurate representation of complex oceanic and biospheric models of anthropogenic carbon uptake. Tellus B 48 (3), 397–417.

Joos, F., Gerber, S., Prentice, I., Otto-Bliesner, B., Valdes, P., 2004. Transient simulations of Holocene atmospheric carbon dioxide and terrestrial carbon since the Last Glacial Maximum. Global Biogeochem. Cycles 18, 1–18.

Jull, M., Mckenzie, D., 1996. The effect of deglaciation on mantle melting beneath Iceland. J. Geophys. Res. 101, 21815–21828.

Jupp, T., Pyle, D., Mason, B., Dade, W., 2004. A statistical model for the timing of earthquakes and volcanic eruptions influenced by periodic processes. J. Geophys. Res. 109(B02206).

Kalnay, E., Kanamitsu, M., Kistler, R., Collins, W., Deaven, D., Gandin, L., Iredell, M., Saha, S., White, G., Woollen, J., et al., 1996. The NCEP/NCAR 40-Year Reanalysis Project. Bulletin of the American Meteorological Society

77 (3), 437–471.

Kennett, J., Thunell, R., 1975. Global increase in Quaternary explosive volcanism. Science 187, 497–503.

Kheshgi, H., 2004. Ocean carbon sink duration under stabilization of atmospheric CO2: A 1,000-year timescale. Geophysical Research Letters 31.

Kohfeld, K., Quere, C., Harrison, S., Anderson, R., 2005. Role of Marine Biology in Glacial-Interglacial CO2 Cycles. Science 308 (5718), 74–78.

Langmuir, C., Klein, E., Plank, T., 1992. Petrological constraints on melt formation and migration beneath mid-ocean ridges. Mantle Flow and Melt Generation at Mid-Ocean Ridges. Geophysical Monograph 71. American Geophysical Union, Washington, 183–280.

Licciardi, J., Kurz, M., Curtice, J., 2007. Glacial and volcanic history of Icelandic table mountains from cosmogenic 3He exposure ages. Quaternary Science Reviews 26 (11-12), 1529–1546.

Licciardi, J., Pierce, K., 2008. Cosmogenic exposure-age chronologies of Pinedale and Bull Lake glaciations in greater Yellowstone and the Teton Range, USA. Quaternary Science Reviews 27 (7-8), 814–831.

Maclennan, J., Jull, M., McKenzie, D., Slater, L., Grönvold, K., 2002. The link between volcanism and deglaciation in Iceland. Geochem. Geophys. Geosyst 3 (11), 1062.

Malinverno, A., 1991. Inverse square-root dependence of mid-ocean-ridge flank roughness on spreading rate. Nature 352 (6330), 58–60.

Manley, W., Kaufman, D., 2002. Alaska PaleoGlacier Atlas: Institute of Arctic and Alpine Research (INSTAAR). University of Colorado v. 1, http://instaar.colorado.edu/QGISL/ak_paleoglacier_atlas.

Marchitto, T., Lynch-Stieglitz, J., Hemming, S., 2005. Deep Pacific CaCO3 compensation and glacial–interglacial atmospheric CO2. Earth and Planetary Science Letters 231 (3-4), 317–336.

Marty, B., Tolstikhin, I., 1998. CO2 fluxes from mid-ocean ridges, arcs and plumes. Chemical Geology 145 (3-4), 233–248.

Mason, B., Pyle, D., Dade, W., Jupp, T., 2004. Seasonality of volcanic eruptions. J. Geophys. Res 109, B04206.

McCulloch, R., Bentley, M., Purves, R., Hulton, N., Sugden, D., Clapperton, C., 2000. Climatic inferences from glacial and palaeoecological evidence at the last glacial termination, southern South America. Journal of Quaternary Science 15 (4), 409–417.

McGuire, W., R., H., C., F., Solow, A., Pullen, S., Saunders, I., I., S., Vita-Finzi, C., 1997. Correlation between rate of seal level change and frequency of explosive volcanism in the Mediterranean. Nature 389, 473–476.

McKenzie, D., 1984. The Generation and Compaction of Partially Molten Rock. Journal of Petrology 25 (3), 713–765.

Monnin, E., Indermuhle, A., Dallenbach, A., Fluckiger, J., Stauffer, B., Stocker, T., Raynaud, D., Barnola, J., 2001. Atmospheric CO2 Concentrations over the Last Glacial Termination.

Monnin, E., Steig, E., Siegenthaler, U., Kawamura, K., Schwander, J., Stauffer, B., Stocker, T., Morse, D., Barnola, J., Bellier, B., et al., 2004. Evidence for substantial accumulation rate variability in Antarctica during the Holocene, through synchronization of CO2 in the Taylor Dome, Dome C and DML ice cores. Earth and Planetary Science Letters 224 (1-2), 45–54.

Montenegro, A., Brovkin, V., Eby, M., Archer, D., Weaver, A., 2007. Long term fate of anthropogenic carbon. Geophys. Res. Lett. 34, L19707.

Nakada, M., Yokose, H., 1992. Ice age as a trigger of active Quaternary volcanism and tectonism. Tectonophysics 212, 321–329.

Neuberg, J., 2000. External modulation of volcanic activity. Geophys. J. Int.

142.

Nowell, D., Jones, C., Pyle, D., 2006. Episodic Quaternary volcanism in France and Germany. J. Quatern. Sci. 21, 645–675.

Rampino, M., Self, S., Fairbridge, R., 1979. Can rapid climate change cause volcanic eruptions? Science 206, 826–828.

Reymer, A., Schubert, G., 1984. Phanerozoic addition rates to the continental crust and crustal growth. Tectonics 3, 63–77.

Saal, A., Hauri, E., Langmuir, C., Perfit, M., 2002. Vapour undersaturation in primitive mid-ocean-ridge basalt and the volatile content of Earth's upper mantle. Nature 419, 451–455.

Saar, M., Manga, M., 2003. Seismicity induced by seasonal ground-water recharge at Mt. Hood, Oregon. Earth Planet. Sci. Lett. 214, 605–618.

Sano, Y., Marty, B., 1995. Origin of carbon in fumarolic gas from island arcs. Chem. Geol. 119, 265–274.

Sano, Y., Williams, S., 1996. Fluxes of mantle and subducted carbon along convergent plate boundaries. Geophys. Res. Lett. 23, 2749–2752.

Schrag, D., Hampt, G., Murray, D., 1996. Pore fluid constraints on the temperature and oxygen isotopic composition of the glacial ocean. Science 272, 1930–1932.

Siebert, L., Simkin, T., 2002. Volcanoes of the world: an illustrated catalog of Holocene volcanoes and their eruptions. Smithsonian Institution, Global Volcanism Program, Digital Information Series, GVP-3.

Sigvaldason, G., Annertz, K., Nilsson, M., 1992. Effect of glacier loading/deloading on volcanism: Postglacial volcanic eruption rate of the Dyngjufjoll area, central Iceland. Bull. Volcanol. 54, 385–392.

Sinton, J., Grönvold, K., Sæmundsson, K., 2005. Postglacial eruptive history of the Western Volcanic Zone, Iceland. Geochem. Geophys. Geosyst 6.

Smith, H. J., Fischer, H., Wahlen, M., Mastroianni, D., Deck, B., 1999. Dual modes of the carbon cycle since the last glacial maximum. Nature 400, 248–250.

Sparks, R., 1981. Triggering of volcanic eruptions by earth tides. Nature 290, 448.

Strogatz, S., 1994. Nonlinear Dynamics and Chaos. Perseus Publishing.

Stuiver, M., Reimer, P., Reimer, R., 2005. CALIB 5.0. WWW program and documentation.

Syracuse, E., Abers, G., 2006. Global compilation of variations in slab depth beneath arc volcanoes and implications. Geochem. Geophys. Geosyst 7.

Thunell, R., Qingmin, M., Calvert, S., Pedersen, T., 1992. Glacial-Holocene biogenic sedimentation patterns in the South China Sea: Productivity variations and surface water pCO2. Paleoceanography 7 (2), 143–162.

Timmermann, A., Timm, O., Stott, L., Menviel, L., in press. The roles of CO_2 and orbital forcing in driving southern hemispheric temperature variations during the last 21,000 years.

Vecsei, A., Berger, W., 2004. Increase of atmospheric CO_2 during deglaciation: Constraints on the coral reef hypothesis from patterns of deposition. Global Biogeochemical Cycles 18 (1).

Walker, J., Hays, P., Kasting, J., 1981. A negative feedback mechanism for the long-term stabilization of Earth's surface temperature. J. of Geophysical Research 86, 9776–9782.

Williams, S., Schaefer, S., et al., 1992. Global carbon dioxide emission to the atmosphere by volcanoes. Geochimica et Cosmochimica Acta 56 (4), 1765–1770.

Wunsch, C., Heimbach, P., 2008. How long to oceanic tracer and proxy equilibrium? Quaternary Science Reviews 27, 637–651.

Yu, Z., Walker, K., Evenson, E., Hajdas, I., 2008. Late glacial and early Holocene climate oscillations in the Matanuska Valley, south-central Alaska. Quaternary Science Reviews 27 (1-2), 148–161.

Zielinksi, G., 2000. Use of paleo-records in determining variability within the volcanism-climate system. Quaternary Science Reviews 19, 417–438.

Zielinksi, G., Mayewksi, P., Meeker, L., Gronvold, K., Germani, M., Whitlow, S., Twickler, M., Taylor, K., 1997. Volcanic aerosol records and tephrochronology of the Summit, Greenland, ice cores. Journal of Geophysical Research 102.